Human and bovine serum albumin, but not mouse serum and egg-white albumin, promote reactivation of viable but non-culturable *Mycobacterium tuberculosis* via the activation of protein kinase-dependent cell division processes

Yuta Morishige[1*], Yoshiro Murase[1], Kinuyo Chikamatsu[1], Hiroyuki Yamada[1], Akio Aono[1], Yuriko Igarashi[1], Keisuke Kamada[1,3], Yoshiko Shimomura[1], Makiko Hosoya[1], and Satoshi Mitarai[1,2]

[1]Department of Mycobacterial Reference and Research, The Research Institute of Tuberculosis, Japan Anti-Tuberculosis Association, Kiyose, Tokyo, Japan.

[2]Department of Basic Mycobacteriology, Graduate School of Biomedical Sciences, Nagasaki University, Nagasaki, Japan.

[3]Department of respiratory medicine, Hokkaido University Hospital, Hokkaido University, Sapporo, Hokkaido, Japan

*** Correspondence:**

Yuta Morishige

ymorishige@jata.or.jp

Keywords: VBNC, Mycobacterium, Albumin, Reactivation, Dormancy

Abstract

We investigated the mechanisms underlying the fetal bovine serum (FBS)-induced reactivation of the viable but non-culturable (VBNC) state of *Mycobacterium tuberculosis* (Mtb) using the H37Rv strain. We found that bovine serum albumin (BSA), a major component of FBS, could

reactivate the VBNC state of Mtb cells without other reactivation-promoting agents. Human serum albumin also had a restorative effect similar to BSA, but mouse serum albumin and egg-white albumin (ovalbumin) did not, suggesting that a common protein structure between bovine and human serum albumin is essential for reactivation. In addition, antioxidative agents, such as N-acetyl-*L*-cysteine, showed no restorative effect, suggesting that the restoration of culturability might not be due to the antioxidative property of BSA. BSA-mediated reactivation is inhibited by H89 and staurosporine. These inhibitors are known to inhibit multiple protein kinases, including serine/threonine protein kinases, in Mtb, suggesting the involvement of mycobacterial protein kinases in cell division during reactivation. These findings provide new insights into the mechanisms of Mtb reactivation, and may contribute to the development of novel strategies for the treatment of latent tuberculosis.

Importance

Reactivation of dormant, including viable but non-culturable (VBNC) *Mycobacterium tuberculosis* (Mtb) cells, represents a critical step in the progression from latent infection to active tuberculosis. However, the molecular mechanisms that trigger this transition are not yet fully understood. We herein report that bovine serum albumin (BSA), a major component of fetal bovine serum, can restore the culturability of VBNC Mtb cells. Human serum albumin showed a similar effect, whereas mouse and egg-white albumins did not, suggesting that the specific structural features shared between bovine and human albumins are essential for reactivation. The lack of reactivation by the antioxidant N-acetyl-*L*-cysteine indicates that the mechanism is not related to redox balance. Inhibition of BSA-induced reactivation by H89 and staurosporine implicates mycobacterial serine/threonine protein kinases in this process. These findings highlight the previously unrecognized role of albumin-kinase signaling in Mtb reactivation and suggest new molecular targets for preventing tuberculosis relapse.

43 **Introduction**

44 *Mycobacterium tuberculosis* (Mtb) develops a latent phenotype, dormancy, due to various
45 stresses, such as host immune response, oxygen depletion, and nutritional starvation, *etc.* The
46 Dormant Mtb cells can persist inside the host and may establish latent tuberculosis infection
47 (LTBI), which requires activation. Lowering the risk of Mtb activation in patients with LTBI
48 is an important strategy to reduce the incidence of TB (1). The viable but nonculturable (VBNC)
49 state is a variant of dormancy in non-sporulating bacteria (2). VBNC cells are a non-culturable
50 population that can be induced by exposure to certain stressors. They cannot grow on nutrient
51 media even after the removal of stress and require a much longer time or specific stimulus for
52 growth (2, 3). It is increasingly being recognized that the VBNC state may play an important
53 role in the survival of Mtb in human hosts.

54 Many pathogenic bacteria, including Mtb, can enter the VBNC state and are considered to be
55 in a protective state in the host environment (4). Various *in vitro* models, such as models of
56 hypoxia, nutritional starvation, a lipid-rich environment, and other multiple stresses, have been
57 reported to induce a VBNC state in Mtb cells (5–9). A deeper understanding of the activation
58 mechanisms of these cells is necessary for the prevention of active tuberculosis.

59 One of the major hypotheses underlying the formation of VBNC bacteria involves the
60 oxidative damage generated by harsh external conditions (10). Some studies have reported that
61 antioxidation during culture is one of the key mechanisms by which VBNC bacteria are
62 reactivated (11, 12). Some mycobacterial culture media containing bovine serum albumin
63 (BSA) and BSA are considered to be involved in the detoxification of growth-suppressing
64 agents that are spontaneously generated during culture (13–15). However, few studies have
65 focused on the effect of such media on the reactivation of VBNC cells or as an antioxidative
66 agent in mycobacterial cultures.

67 Previously, the NADH oxidase inhibitor diphenyleneiodonium chloride (DPI) was reported

68 to simply and rapidly induce a VBNC state in Mtb H37Ra, and incubation with fetal bovine
69 serum (FBS) facilitated the reactivation of VBNC cells, whereas incubation with oleic-
70 albumin-dextrose-catalase (OADC) supplementation did not (16). This report provides
71 important clues for constructing a simple and rapid assay system to reactivate VBNC Mtb cells.
72 However, we found that the whole body of FBS might not be essential for the reactivation of
73 DPI-induced H37Rv VBNC cells, but the presence of BSA, a major component of FBS, seemed
74 to be sufficient to reactivate the VBNC state, as observed for both H37Rv and H37Ra. Because
75 FBS contains a high concentration of BSA, we hypothesized that BSA would act as a
76 reactivation-promoting agent for DPI-induced VBNC cells.

77 One possible reactivation mechanism of BSA is its antioxidative properties, which have been
78 well studied (17). Another possibility is cellular processes involving cAMP, an important
79 second messenger in the cell. Shleeva *et al*. showed that the presence of high amounts of cAMP
80 provided by adenylyl cyclase is essential for the reactivation of *M. smegmatis* and Mtb from
81 the VBNC state (18, 19). Notably, overexpression of Rv*2212* gene, which encodes adenylyl
82 cyclase in Mtb (20), significantly affects both entry into and reactivation from the VBNC
83 state (19).

84 Understanding the detailed reactivation mechanism of VBNC is crucial for reducing the risk
85 of Mtb disease development. In this study, we reported that the reactivation-promoting
86 mechanisms of BSA against DPI-induced VBNC Mtb might not be due to its antioxidative
87 property or the activation of adenylyl cyclase.

88 Results

89 I. DPI treatment induced a VBNC state in Mtb H37Rv

90 Yeware *et al.* previously reported that DPI treatment, which inhibits the electron transport
91 system, resulting in the inhibition of aerobic respiration, could effectively induce the VBNC

92 state in Mtb H37Ra cells (16). In our study, we confirmed that H37Ra and H37Rv cells could
93 effectively enter the VBNC state with DPI treatment, as evaluated by culturability, loss of acid-
94 fastness, and accumulation of neutral lipids. Figure 1 shows the DPI treatment results for the
95 induction of the VBNC state in H37Rv cells. As shown in Fig. 1(A), the numbers of culturable
96 cells in the untreated control population and DPI-treated population were significantly
97 different: $4.43 \pm 1.43 \times 10^8$ CFU/mL for the untreated control population and $4.64 \pm 6.10 \times 10^3$
98 CFU/mL for the DPI-treated population ($p = 0.033$). Fig. 1(B) shows that the proportion of
99 CFDA-positive cells in the untreated control and DPI-treated populations was not significantly
100 different (81.8 ± 11.4% vs 65.9 ± 11.8%, $p = 0.169$). Representative images of CFDA/EtBr
101 dual-stained cells from the untreated control and DPI-treated populations are shown in Fig.
102 1(C). These results indicate that the majority of DPI-treated H37Rv cells were alive, while their
103 culturability deteriorated significantly.

104 Auramine-O/Nile Red dual staining showed a reduction in acid fastness and accumulation
105 of neutral lipids. As shown in Fig. 1(D), the proportion of acid-fast-negative/lipid
106 accumulation-positive cells was 84.0 ± 14.0% in the DPI-treated population, and 12.1 ± 11.9%
107 in the untreated control population ($p < 0.01$). Representative images of auramine-O/Nile Red
108 dual-stained cells in the untreated control and DPI-treated populations also showed distinctive
109 differences in the proportions of acid-fast-positive cells and lipid-accumulation-positive cells
110 (Fig. 1[E]). The loss of acid-fastness was also confirmed by Ziehl-Neelsen staining; the
111 majority of DPI-treated populations were found to have lost their acid-fastness (Suppl. Fig. 1).
112 Interestingly, Airyscan microscopy revealed that some DPI-treated cells were positive for acid-
113 fast and neutral lipid staining, suggesting the presence of cells in the transitional state from
114 culturable to VBNC (Fig. 1[F]). These results indicate that DPI treatment induced the VBNC
115 state in H37Rv and H37Ra.

116 **II. BSA is essential on the reactivation of DPI-induced VBNC Mtb cells.**

117 To evaluate whether DPI-treated H37Rv cells could regain culturability by supplementing
118 the medium with FBS, we performed a reactivation assay on DPI-treated H37Rv cells
119 supplemented with FBS or OADC. As shown in Fig. 2(A) and (B), our results partially support
120 the previous study (16) with some differences; not only were the DPI-treated H37Rv cells
121 reactivated by incubation with FBS-supplemented medium, but also the OADC-supplemented
122 medium. Addition of albumin alone to the medium can also induce reactivation. The addition
123 of FBS to the BSA-free Dubos medium slightly reduced the regrowth rate; however, cells were
124 successfully reactivated at the end of incubation with or without FBS. This phenomenon was
125 also observed for H37Ra (Suppl. Fig. 2). Thus, we used H37Rv for further analyses in this
126 study.

127 Incubation with sodium pyruvate, which has been reported to have a reactivation-promoting
128 effect on VBNC cells elsewhere (21–23), led to transient regrowth by day 15 and a slight
129 reduction at day 20. (Suppl. Fig. 3[A] and [B]).

130 We also confirmed that the growth rates under the two conditions did not differ significantly
131 (p = 0.428 on day 5, Suppl. Fig. 4[A]). Supplementary Figure 4(B) also shows sufficient cell
132 growth. The cells were more aggregative without BSA; however, aggregation was easily
133 dispersed by pipetting, and there was no significant difference in the OD_{600} value. Albumin is
134 not essential for Mtb growth.

135 III. Reactivation-promoting effect by BSA is not attributed to its antioxidative 136 property.

137 It is well known that antioxidants are effective as reactivation-promoting agents for bacteria
138 in the VBNC state (3). We hypothesized that the reactivation-promoting effect of BSA might
139 be due to its antioxidative properties and assumed that human serum albumin (HSA), which
140 has a similar structure, and ovalbumin (OVA), which has a different structure but a stronger

141 antioxidative effect, as well as NAC (antioxidant) and D-mannitol (free radical scavenger),
142 would also reactivate VBNC Mtb. As shown in Fig. 3(A) and (B), the reactivation-promoting
143 effect of albumin was specific to BSA and HSA. Contrary to our expectation, OVA did not
144 show a reactivation-promoting effect but maintained the number of culturable cells in this
145 system. Contrary to our expectations, neither NAC nor D-mannitol showed reactivation-
146 promoting activity.

147 Interestingly, we found that mouse serum albumin (MSA) did not show a reactivation
148 promoting effect (Suppl. Fig. 5). Although only a subset of commercially available species was
149 analyzed, these results suggest that the reactivation promoting effect of serum albumin on DPI-
150 treated Mtb may be specific to certain mammalian species.

151 We also checked whether the purity of albumin affected the promotion of reactivation using
152 fatty acid- and globulin-free BSA and confirmed that there was no significant difference (p =
153 0.986) in the reactivation-promoting effects (Suppl. Fig. 6). These results suggest that
154 commercially available albumin, including fatty acids, does not affect reactivation of DPI-
155 treated Mtb.

156

157 **IV. The reactivation-promoting effect of albumin was canceled by treatment with**
158 **eukaryotic protein kinase inhibitor.**

159 As Shleeva *et al.* reported that cAMP production from adenylyl cyclase is essential for the
160 reactivation of VBNC Mtb (18), we hypothesized that the inhibition of adenylyl cyclase and its
161 downstream enzyme, protein kinase, could modulate the reactivation-promoting effect of BSA.
162 As shown in Fig. 4(A) and (B), SQ22536, an adenylyl cyclase inhibitor, only suppressed
163 reactivation at a very high concentration (10 mM). In contrast, H89, a eukaryotic protein kinase
164 inhibitor, suppressed reactivation in a dose-dependent manner. In detail, incubation with 10
165 μM or 30 μM H89 resulted in a CFU/mL value for $3.42 \times 10^6 \pm 7.45 \times 10^5$ CFU/mL and 3.63

166 ± 1.70 × 10^2 CFU/mL, while incubation without H89 resulted in 3.00 × 10^8 ± 5.07 × 10^7
167 CFU/mL. We also confirmed that staurosporine, a known mycobacterial protein kinase PknB
168 inhibitor (24), suppressed reactivation at a concentration of 10 μM and resulted in a CFU/mL
169 value of 2.09 × 10^3 ± 7.62 × 10^2 CFU/mL, whereas incubation without staurosporine resulted
170 in 3.58 × 10^8 ± 5.78 × 10^7 CFU/mL (Fig. 4[A] and [B]). None of the inhibitors used in this
171 study reduced the growth of intact Mtb cells (Suppl. Fig. 7A and 7B).
172 Since both SQ22536 and H89 are targeted to eukaryotic enzymes, we also performed a
173 molecular docking simulation of these inhibitors against their equivalent targets on Mtb to
174 validate the inhibition assay. As shown in Supplemantary Table 1, SQ22536 and H89 have
175 sufficient affinity for Rv2212 (adenylyl cyclase) and PknA (protein kinase), respectively.

176 **Discussion**

177 In this study, we found that BSA, a supplement to mycobacterial culture, could act as a
178 reactivation-promoting agent of the VBNC state of Mtb. We also showed that this effect of
179 serum albumin might be species-specific: bovine and human serum albumin had the effect,
180 while mouse serum albumin did not. The predictive mechanism of BSA-induced reactivation
181 was also proposed to involve the activation of mycobacterial protein kinase, not its
182 antioxidative property or the activation of adenylyl cyclase.
183 The mechanism underlying the effect of DPI is thought to involve the inhibitory effect of
184 NADH oxidase, which results in inhibition of the electron transport system of Mtb. This may
185 induce an unbalanced NADH/NAD ratio and hypoxic response in liquid culture, resulting in a
186 significant decrease in culturability (Fig. 1[A]) (16). However, viability was highly retained
187 (65.9%), suggesting that the majority of the cells were transformed into VBNC (Fig. 1[B]).
188 VBNC transformation was confirmed by auramine-O and Nile Red staining. The loss of acid-
189 fastness and accumulation of neutral lipids are distinctive features of VBNC mycobacterial
190 cells.

191 Our data also demonstrated that the majority of DPI-treated Mtb H37Rv cells were stained
192 with Nile Red alone (Fig. 1[D]). Airyscan super-resolution microscopy showed the presence of
193 cells stained with auramine-O, which contained an intracellular lipid body stained with Nile
194 Red (Fig. 1[F]). This could also reveal the distribution of the lipid body in the cell as some foci
195 of relatively strong signals of Nile Red, suggesting a transformation from a growing state to
196 VBNC, with drastic alterations in lipid metabolism.

197 We also found that DPI-induced VBNC could facilitate reactivation not only by incubation
198 with FBS, but also with OADC supplementation and BSA alone, suggesting that albumin might
199 act as a reactivation-promoting agent in both H37Rv and H37Ra (Fig. 2 and Suppl. Fig. 2).
200 These findings were contrary to those of a previous study, which showed that only FBS can
201 facilitate reactivation (16). We considered that the reason for this difference may be due to a
202 contaminant in Tween 80: the presence of an excessive amount of oleic acid. We also
203 confirmed that reactivation was not facilitated by the use of prediluted Tween 80 for the
204 preparation of Dubos medium (unpublished data) for both H37Rv and H37Ra, probably due to
205 extended hydrolyzation of Tween 80 (25). Thus, our results suggest that the key reactivation-
206 promoting agent in FBS is serum albumin, and further analyses were performed using H37Rv.

207 It should be noted that not all cells completely transitioned to the VBNC state in this study.
208 In general, *in vitro* cultured cells are thought to be a non-uniform population due to the
209 difference in microenvironment; oxygen concentration and nutritional conditions might vary
210 at the local level, which could make the variable subpopulations in metabolic state, as Yeware
211 *et al.* also indicated (16). In our study, a small subpopulation (10^3 CFU/mL) was found that
212 could not proliferate on Dubos broth without BSA but could proliferate on agar medium (Fig.
213 2). The results of acid-fast staining also suggested the presence of cells that appeared to be in
214 the process of transitioning from a culturable state to a VBNC state (Fig. 1F). These results
215 suggest that, although the VBNC state could be induced by DPI treatment, the level of
216 induction might vary from cell to cell. Therefore, the results of an *in vitro* VBNC model should

217 be carefully interpreted and the final conclusions must be verified in *in vivo* model with
218 albumin administration.

219 Our results showed that the reactivation-promoting effect of albumin might be structure-
220 specific because OVA did not facilitate reactivation, whereas BSA and HSA did. Regarding
221 their amino acid sequences, BSA and HSA share 76% sequence homology (26); however, BSA
222 and OVA share less sequence homology (16%). One of the considerable roles of albumin is as
223 an antioxidative agent because of its cysteine residues with free thiols (17, 27). BSA and HSA
224 have only one cysteine residue with a free thiol, whereas OVA has four cysteines with free
225 thiols (28). Although OVA therefore seems to be more reductive than BSA and HSA, their
226 reactivation-promoting effect is paradoxical, indicating that antioxidative properties might not
227 be essential for this effect. This hypothesis was considered to support the reduced effect of
228 NAC and D-mannitol. Moreover, this paradoxical result confirmed that certain common
229 structures of BSA and HSA may be essential. Additionally, we would like to note that MSA
230 did not show the reactivation promoting effect, suggesting that this effect might have species-
231 dependency (Suppl. Fig. 5). At this point, we have found that there are certain differences
232 between bovine and mouse serum albumins (internal data) and analyzed their contribution to
233 this property for the subsequent study, including measurement of the reactivation-promoting
234 effect of MSA on VBNC *M. microti*, a pathogen of small field rodents (29). These results
235 suggest that the effect of albumin may be due to its complex functions rather than antioxidative
236 properties.

237 Serum albumin is known to act as a good carrier for many biologically active substances,
238 including free fatty acids. It is also known as a detoxifier of growth-arresting substances in
239 culture medium. BSA is added to the mycobacterial culture medium as both a carrier and
240 detoxifier of growth-supporting and growth-arresting substances, respectively. Shleeva *et al*.
241 showed that several types of unsaturated free fatty acids, including oleic, linoleic, and
242 arachidonic acids, can promote the reactivation of VBNC *M. smegmatis* in modified Sauton's

243 medium, and oleic acid also works in Mtb (18). It should be noted that albumin impurities did
244 not affect reactivation in this study. Although the underlying mechanism is still unclear, both
245 fatty acid- and globulin-free BSA and BSA Cohn fraction V showed a similar reactivation-
246 promoting effect toward DPI-treated Mtb (Suppl. Fig. 6).

247 The reactivation inhibition assay using SQ22536, H89, and staurosporine provided an
248 important clue for understanding the effect of BSA. In the present study, we suppressed the
249 reactivation of DPI-induced VBNC cells by inhibiting adenylyl cyclase at a very high
250 concentration of SQ22536. Although the underlying mechanism is unclear, adenylyl cyclase
251 may not play a key role in reactivation from a DPI-induced VBNC state, whereas the inhibition
252 of protein kinase by H89 and staurosporine clearly suppressed reactivation. These results
253 suggest that protein kinase might be involved in the reactivation of VBNC Mtb cells triggered
254 by BSA, and that the contribution of adenylyl cyclase may be smaller than that of protein kinase.

255 Mtb encodes eukaryotic Ser/Thr protein kinases including PknA, PknB, and PknD-L.
256 Among them, PknA regulates major cell processes, regulates several types of proteins involved
257 with mycobacterial cell division and morphogenesis via phosphorylation of such proteins in
258 coordination with PknB (30, 31); phosphorylation of GlmU (Rv*1018c*) and MurD (Rv*2155c*),
259 Wag31 (Rv*2145c*), HupB (Rv*2986c*) and ParB (Rv*3917c*), influence the production and cross-
260 linking of peptidoglycan precursors (32–35), the spatial localization of peptidoglycan
261 synthesis(36), DNA condensation and partitioning (37, 38), respectively. Notably, the
262 phosphorylation of FtsZ and FipA by PknA controls cell division under oxidative stress(39, 40).
263 In addition, mycobacterial protein kinase has cyclic AMP-dependent protein kinase domains,
264 which are very similar to the eukaryotic version, which was shown in PknB (41), and
265 staurosporine, which acts as a PknB inhibitor, could also inhibit the reactivation of DPI-induced
266 VBNC Mtb (Fig. 4).

267 Our study suggests that the inhibition of mycobacterial protein kinase by H89 and
268 staurosporine critically affects several important cellular processes that underlie reactivation

269 (Suppl. Fig. 8). To confirm the role of mycobacterial protein kinases and related proteins in the
270 reactivation of DPI-induced VBNC cells by albumin, further studies involving gene
271 knockdown using CRISPR interference (CRISPRi) (42) are necessary. This is particularly
272 relevant because most of these proteins, except FipA (Rv*0019c*), are essential for *in vitro*
273 growth; (43–46) therefore, genetic manipulation using conventional methods is not permissible.

274 **Conclusion**

275 Our data showed that the presence of BSA in Dubos medium not only depleted growth-
276 suppressing substances, but also triggered the reactivation of the DPI-induced VBNC state in
277 both H37Rv and H37Ra strains. The reactivation-promoting effects of other kinds of albumins
278 and antioxidative agents, including NAC and D-mannitol, were tested; however, only bovine
279 and human serum albumin showed a reactivation-promoting effect. The results of the inhibition
280 assay of reactivation using SQ22536, H89, and staurosporine suggest that the inhibition of
281 mycobacterial protein kinase suppressed reactivation to a much greater extent than adenylyl
282 cyclase, indicating the presence of a reactivation-promoting protein kinase-dependent pathway.
283 To the best of our knowledge, few studies have focused on the reactivation-promoting effects
284 of albumin on VBNC Mtb. Taken together, our findings indicated that the reactivation of Mtb
285 from a DPI-induced VBNC state could be obtained by interaction with bovine serum albumin
286 and the mechanism of albumin-induced reactivation may involve the activation of
287 mycobacterial protein kinase, which regulates several important processes of cellular
288 component construction and cell division. Although it remains unclear how albumin interacts
289 with VBNC cells, our study provides some important clues for understanding the physiology
290 of the mycobacterial VBNC state.

291 **Author Contributions**

292 YMori, YMura, and SM conceived and designed the experiments. Y. Mori performed the

experiments. YMura, KC, AA, YI, YS, MH, KK, HY, AT, and SM assisted with the experiments. YMori acquired the data, and YMori and YMura analyzed the data. YMori performed a molecular docking simulation and statistical analysis. YMori, YMura, and SM wrote the manuscript. All authors have contributed to the manuscript and approved the submitted version.

Data availability

All data contained in this study can be obtained from the corresponding author upon reasonable request.

Funding

This work was supported by the Research Program on Emerging and Re-emerging Infectious Diseases of the Japan Agency for Medical Research and Development (AMED), Grant-in-Aid for Early-Career Scientists, and Grant-in-Aid for Scientific Research (C) from the Japan Society for the Promotion of Science (JSPS) KAKENHI. The grant numbers are JP21fk0108090, 21K15442, and 24K10228.

Acknowledgments

The authors thank Dr. K. Suenaga and Mr. H. Sakuma (Carl Zeiss Co., Ltd., Tokyo, Japan) for their assistance in obtaining super-resolution images. The authors also thank Dr. A. Osugi (Research Institute of Tuberculosis, Japan Anti-Tuberculosis Association) for the valuable discussions. The authors also thank Dr. Brian Quinn (Japan Medical Communication). Inc.) for their help with the preparation of this manuscript.

Conflict of Interest Statement

314 The authors declare that the research was conducted in the absence of any commercial or
315 financial relationships that could be construed as potential conflicts of interest.

316

317 **Materials and Methods**

318 **Bacterial strains, growth media and culture conditions**

319 This study was carried out using *Mycobacterium tuberculosis* H37Rv (ATCC 27294) and
320 H37Ra (ATCC 25177). Both cells were cultured for 3–5 days in a 60 mL glycol-modified
321 polyethylene terephthalate (PETG) bottle containing 20 mL Dubos broth (2.5 g/L Na_2HPO_4,
322 2.0 g/L L-asparagine, 1.0 g/L KH_2PO_4, 0.5 g/L pancreatic digest of casein, 0.2 g/L Tween 80,
323 0.5 mg/mL $CaCl_2$•$2H_2O$, 0.1 mg/mL $CuSO_4$, 0.1 mg/mL $ZnSO_4$•$7H_2O$, 0.05 g/L ferric
324 ammonium citrate, 0.01 g $MgSO_4$•$7H_2O$) with 5% (v/v) glycerol, and 10% (v/v) ADC
325 supplementation (5.0 g bovine serum albumin fraction V (BSA), 2.0 g dextrose, 0.003 g
326 catalase in 100 mL distilled water) at 37˚C in an orbital shaker (100 rpm) until the OD_{600}
327 reached up to 0.35. All procedures were performed at a BSL-3 facility. For further analysis, we
328 used commercially available BSA Cohn fraction V (Merck, Darmstadt, Germany) unless
329 otherwise stated. In addition, we used molecular biology grade Tween 80 (Merck product
330 number P5188-100ML) without predilution.

331 **Counting the number of culturable cells**

332 The cultured bacterial suspension was serially diluted 10-fold in phosphate buffered saline (pH
333 6.8) with 0.1% (w/v) Tween 80 (PBS-T) and 25 µL of each diluent was inoculated onto a
334 Middlebrook 7H10 agar plate supplemented with oleic-albumin-dextrose-catalase (OADC)
335 (Becton Dickinson, Sparks, MD) in duplication. Colonies were counted after at least three
336 weeks of incubation at 37 °C under 5% CO_2. The limit of detection was determined to be 20
337 CFU/mL owing to the diluent factor.

338 **Effect of BSA on the growth of Mtb cells in Dubos medium**

339 Ten milliliters of log phase culture of Mtb H37Rv (OD_{600} = 0.35) in Dubos medium, as
340 described previously, was sedimented at 3,000 ×*g* for 10 min at 4 °C, and the supernatant was
341 discarded. The sediment was washed twice with fresh Dubos broth and resuspended in 10 mL
342 Dubos broth. The suspension was diluted 1:10 with Dubos broth with or without the addition
343 of BSA solution (5.0 g BSA fraction V in 100 mL distilled water) at a final concentration of
344 0.1% (w/v) BSA. The diluted suspension was dispensed into 24-well plates (Sarstedt,
345 Nümbrecht, Germany) in 1.5 mL increments and sealed with gas-permeable film (Breathe-Easy,
346 Diversified Biotech Inc, Dedham, MA, United States). Cultures were incubated for 5, 10, 15,
347 and 20 days at 37 °C under 5% CO_2. At each time point, the number of culturable cells was
348 measured, as described above.

349 **Induction of the VBNC cells**

350 Induction of the VBNC cells was performed according to a previous report (16) with some
351 modifications. In short, the log phase culture of Mtb H37Rv or H37Ra (OD_{600} = 0.35) in Dubos
352 medium was evenly divided into 30 mL PETG bottles, and 5 mg/mL diphenyleneiodonium
353 chloride (DPI) in dimethyl sulfoxide (DMSO) solution was directly added at a final
354 concentration of 4 µg/mL with immediate agitation. An equal volume of DMSO was added to
355 the untreated control samples. The cultures were incubated for 24 h at 37 °C without shaking.
356 After incubation, their culturability and viability were measured as described above.

357 **Cell viability assay**

358 Mtb cells was measured by esterase activity and membrane integrity of the cells using dual
359 staining with 10 mg/mL carboxyfluorescein diacetate (CFDA, DOJINDO LABORATORIES,
360 Kumamoto, Japan) and ethidium bromide (EtBr, DOJINDO LABORATORIES). Briefly, 500
361 µL of DPI-treated or untreated Mtb culture was sedimented by centrifugation at 15,000 ×*g* for
362 5 min at 4 °C and washed twice with an equal volume of PBS-T. The washed bacterial sediment

363 was resuspended in 200 μL of PBS-T with CFDA and EtBr and incubated at room temperature
364 (RT) for 30 min in the shade. The final concentrations of CFDA and EtBr were 60 μg/mL and
365 2 μg/mL, respectively. Stained Mtb cells were washed twice with PBS-T and fixed with 3.7%
366 formaldehyde solution at RT for at least 2 h. After fixation, 10 μL of the bacterial suspension
367 was smeared on three APS-coated 8-well slides (Matsunami Glass, Osaka, Japan) and air-dried.
368 The slides were then mounted with DPX new non-aqueous mounting medium (Merck,
369 Darmstadt, Germany) and a 150 μm thick cover glass (Matsunami glass, Osaka, Japan) prior
370 to microscopic observation. Specimens were examined using a BX53 fluorescence microscope
371 (Olympus, Tokyo, Japan) with a 100× objective lens for green (esterase-active with intact
372 membrane; live) or red (esterase-negative with damaged membrane; dead) fluorescing cells.
373 At least 10 random fields were observed for each sample and the images (TIFF format) were
374 analyzed using the Fiji/ImageJ software program(47). The live/dead ratio was calculated by
375 directly counting green or red fluorescent cells.

376 **Auramine-O/Nile Red dual staining**

377 Loss of acid fastness and accumulation of neutral lipids are distinctive features of VBNC
378 mycobacteria(48). To detect the phenotype, fluorescent acid-fast staining with auramine-O and
379 neutral lipid staining with Nile Red (9-dimethylamino-5H-benzo-α-phenoxadine-5-one) were
380 performed using a previously described method (9) with some modifications. Ten microliters
381 of DPI-treated or untreated cultures were smeared onto an APS-coated slide (Matsunami Glass,
382 Osaka, Japan) and air-dried. The slides were then heat-fixed and cooled to room temperature
383 before staining. The smear was flooded with fluorochrome staining solution (10 μg/mL
384 auramine-O in 5% [w/v] phenol solution) and incubated at room temperature for 20 min in the
385 dark. The excess dye was removed using 3% hydrochloric acid in ethanol for 15 min. The
386 smear was then covered with 10 μg/mL Nile Red in ethanol and incubated at room temperature
387 for 15 min. Finally, the smear was counterstained with a 0.1% (w/v) potassium permanganate

388 solution for 1 min. The stained slides were air-dried and mounted, as previously described.
389 Fluorescence microscopy was performed with a 100× objective lens for green (acid-fastness
390 positive, lipid accumulation negative; active) or red (acid-fastness negative, lipid accumulation
391 positive; VBNC) fluorescent cells. At least five random fields were observed for each sample,
392 and images (TIFF format) were analyzed using the Fiji/ImageJ software program.(47) The
393 proportion of acid-fast-positive cells and lipid-accumulation-positive cells was calculated by
394 direct counting of green or red fluorescent cells.

395 **Acid-fast staining**

396 Ziehl-Neelsen staining was also performed to confirm the loss of acid-fastness resulting in the
397 VBNC state by DPI treatment, according to the standard method(49). The slides were observed
398 under a light microscope with a 100× objective lens (BX53, Olympus, Tokyo, Japan).

399 **Confocal super-resolution microscopy**

400 Detailed images of accumulated lipids were obtained using a confocal laser-scanning
401 microscope (LSM900 with Airyscan 2, Carl Zeiss Microscopy, Jena, Germany). Briefly, culture
402 slides of DPI-treated cells dual-stained with auramine-O and Nile Red, as described above,
403 were observed with a 63× objective lens. The green fluorescence emission from auramine-O
404 and red fluorescence from Nile Red were sequentially collected using a variable dichroic beam
405 splitter and an Airyscan 2 detector. Super-resolution images were processed using ZEN Blue
406 software (Carl Zeiss, Jena, Germany).

407 **VBNC reactivation assay**

408 The VBNC reactivation assay was performed as described previously (16) with some
409 modifications. DPI-treated cultures were sedimented by centrifugation at 3,000 x*g* for 10 min
410 at 4 °C, washed twice with fresh Dubos broth, and resuspended in ten-milliliters of Dubos broth.
411 The bacterial suspension was diluted 1:10 with fresh Dubos medium, with or without 0.1%

412 (w/v) BSA. For both the BSA-containing and BSA-free series, OADC supplementation
413 (Becton Dickinson, Sparks, MD, USA), fetal bovine serum (FBS; Moregate BioTech, Bulimba,
414 Queensland, Australia), or sodium pyruvate (PA; Merck) were added. The final concentration
415 of each reagent was 10% (v/v) for OADC supplementation, 2% (v/v) for FBS, and 3 mM for
416 PA. The diluted suspension was then dispensed into 24-well plates in 1.5 mL increments and
417 sealed with a gas-permeable film. Cultures were incubated for 5, 10, 15, and 20 days at 37 °C
418 under 5% CO_2. At each time point, the number of culturable cells was measured, as previously
419 described.

420 **Evaluation of the reactivation-promoting effect of human and mouse serum albumin, egg-**
421 **white albumin (ovalbumin) and antioxidative agents**

422 To determine whether the reactivation-promoting effect of BSA is its antioxidative property,
423 we measured the reactivation-promoting activity of other albumins that have variable
424 antioxidative properties and antioxidative agents toward DPI-treated Mtb cells. Washed DPI-
425 treated cells were resuspended in fresh Dubos broth without BSA, and the suspension was
426 diluted 1:10 with Dubos broth containing BSA, human serum albumin (HSA), mouse serum
427 albumin (MSA), ovalbumin (OVA), N-acetyl-*L*-cysteine (NAC), or D-mannitol (MAN). The
428 final concentration of each reagent was 0.1% (w/v) for BSA, HSA, MSA, and OVA; 500 μM
429 for NAC; and 50 mM for MAN. The subsequent reactivation assay was performed according
430 to the method described above.

431 **Evaluation of the reactivation-promoting effect of fatty acid and globulin-free BSA**

432 To determine the effect of BSA Cohn fraction V contaminants, we measured the reactivation-
433 promoting activity of fatty acid and globulin-free BSA toward DPI-treated VBNC Mtb cells.
434 Washed DPI-treated cells were resuspended in fresh Dubos broth without BSA, and the
435 suspension was diluted 1:10 with Dubos broth containing BSA Cohn fraction V or fatty acid
436 and globulin-free BSA. Fatty acid and globulin-free BSA were acquired from Merck. The final

437 concentration of both the BSAs was 0.1% (w/v). The subsequent reactivation assay was
438 performed according to the method described above.

439 **Effects of adenylyl cyclase or protein kinase on BSA-induced reactivation**

440 Washed DPI-treated VBNC Mtb cells were resuspended in fresh Dubos broth, and the
441 suspension was diluted to 1:10 with Dubos broth containing 0.1% (w/v) BSA containing
442 adenylyl cyclase inhibitor SQ22536 (Merck, Darmstadt, Germany), protein kinase inhibitor
443 H89 (Abcam, Cambridge, United Kingdom), or staurosporine (Merck). The final
444 concentrations of each inhibitor were as follows: 0.1 to 10 mM SQ22536, 1–30 μM H89 and 1
445 to10 μM for staurosporine. The number of culturable cells was then measured as described
446 previously.

447 **Molecular docking simulation**

448 Molecular docking simulation was performed using the AutoDock Vina software program
449 (version 1.1.2), an open-source molecular docking program designed by the Scripps Research
450 Institute(50, 51). The 3D structures of the receptor proteins PknA and Rv*2212* were obtained
451 from the Protein Data Bank (52) and AlphaFold Database(53, 54), respectively. The PDB ID for
452 PknA was 4OW8 (55) and the AlphaFold Database identifier for Rv*2212* was AF-P9WMU7-
453 F1. We removed water molecules from the proteins, added polar hydrogen and charge, and
454 adjusted the X-Y-Z coordinates and grid size to optimize molecular docking. Each simulation
455 was performed using default options. The 3D structures of the ligand molecules, H89, SQ22536
456 and ATP were obtained from the PubChem Database. The PubChem CIDs of the ligands were
457 449241, 5270, and 5957, respectively. Graphical processing was performed using the UCSF
458 Chimera software program version 1.16(56).

459 **Statistical analysis**

460 The statistical significance of differences between culturable cell counts of Mtb cells in

untreated and DPI-treated cells was determined by Student's *t*-test. The statistical significance of differences between staining of Mtb cells in untreated and DPI-treated cells was determined using Welch's *t*-test. The statistical significance of differences between culturable cell counts of DPI-treated Mtb cells at days 0 and 20 on reactivation was determined by the Student's *t*-test. For multiple group comparisons, one-way analysis of variance (ANOVA) was performed, followed by Tukey's honest significant difference (HSD) test for multiple comparisons. Only comparisons with the control group (day 0) were extracted. Statistical analysis was performed with R (57) using EZR in the R package(58). $P < 0.05$.

References

1. World Health Organization. 2020. TB disease burden, p. 23. *In* Global Tuberculosis Report 2020 Chapter 4. World Health Organization.

2. Ayrapetyan M, Williams T, Oliver JD. 2018. Relationship between the Viable but Nonculturable State and Antibiotic Persister Cells. Journal of Bacteriology 200.

3. Li L, Mendis N, Trigui H, Oliver JD, Faucher SP. 2014. The importance of the viable but non-culturable state in human bacterial pathogens. Frontiers in Microbiology https://doi.org/10.3389/fmicb.2014.00258.

4. Oliver JD. 2010. Recent findings on the viable but nonculturable state in pathogenic bacteria. FEMS Microbiology Reviews 34:415–425.

5. Wayne LG, Hayes LG. 1996. An in vitro model for sequential study of shiftdown of *Mycobacterium tuberculosis* through two stages of nonreplicating persistence. Infection and immunity 64:2062–9.

6. Betts JC, Lukey PT, Robb LC, McAdam RA, Duncan K. 2002. Evaluation of a nutrient starvation model of *Mycobacterium tuberculosis* persistence by gene and protein expression profiling. Molecular microbiology 43:717–31.

7. Salina EG, Waddell SJ, Hoffmann N, Rosenkrands I, Butcher PD, Kaprelyants AS. 2014. Potassium availability triggers *Mycobacterium tuberculosis* transition to, and resuscitation from, non-culturable

(dormant) states. Open Biology 4:140106.

8. Aguilar-Ayala DA, Cnockaert M, Vandamme P, Palomino JC, Martin A, Gonzalez-Y-Merchand J. 2018. Antimicrobial activity against *Mycobacterium tuberculosis* under in vitro lipid-rich dormancy conditions. Journal of medical microbiology 67:282–285.

9. Deb C, Lee CM, Dubey VS, Daniel J, Abomoelak B, Sirakova TD, Pawar S, Rogers L, Kolattukudy PE. 2009. A novel in vitro multiple-stress dormancy model for *Mycobacterium tuberculosis* generates a lipid-loaded, drug-tolerant, dormant pathogen. PLoS ONE 4:e6077.

10. Desnues B, Cuny C, Grégori G, Dukan S, Aguilaniu H, Nyström T. 2003. Differential oxidative damage and expression of stress defence regulons in culturable and non-culturable *Escherichia coli* cells. EMBO reports 4:400–404.

11. Imazaki I, Nakaho K. 2009. Temperature-upshift-mediated revival from the sodium-pyruvate-recoverable viable but nonculturable state induced by low temperature in *Ralstonia solanacearum*: linear regression analysis. Journal of General Plant Pathology 2009 75:3 75:213–226.

12. Mizunoe Y, Wai SN, Ishikawa T, Takade A, Yoshida S. 2000. Resuscitation of viable but nonculturable cells of *Vibrio parahaemolyticus* induced at low temperature under starvation. FEMS Microbiology Letters 186:115–120.

13. Lynn M, Wilson AR, Solotorovsky M. 1979. Role of bovine serum albumin in the nutrition of *Mycobacterium tuberculosis*. Applied and Environmental Microbiology 38:806–810.

14. Dubos RJ. 1947. THE EFFECT OF LIPIDS AND SERUM ALBUMIN ON BACTERIAL GROWTH. The Journal of experimental medicine 85:9–22.

15. Davis BD, Dubos RJ. 1947. THE BINDING OF FATTY ACIDS BY SERUM ALBUMIN, A PROTECTIVE GROWTH FACTOR IN BACTERIOLOGICAL MEDIA. The Journal of experimental medicine 86:215–228.

16. Yeware A, Gample S, Agrawal S, Sarkar D. 2019. Using diphenyleneiodonium to induce a viable but non-culturable phenotype in *Mycobacterium tuberculosis* and its metabolomics analysis. PLoS ONE 14:e0220628.

17. Roche M, Rondeau P, Singh NR, Tarnus E, Bourdon E. 2008. The antioxidant properties of serum albumin. FEBS Letters 582:1783–1787.

18. Shleeva M, Goncharenko A, Kudykina Y, Young D, Young M, Kaprelyants A. 2013. Cyclic amp-dependent resuscitation of dormant mycobacteria by exogenous free fatty acids. PLoS ONE 8:e82914.

19. Shleeva MO, Kondratieva TK, Demina GR, Rubakova EI, Goncharenko A V., Apt AS, Kaprelyants AS. 2017. OVerexpression Of adenylyl cyclase encoded by the *Mycobacterium tuberculosis* Rv2212 gene confers improved fitness, accelerated recovery from dormancy and enhanced virulence in mice. Frontiers in Cellular and Infection Microbiology 7:370.

20. Knapp GS, Lyubetskaya A, Peterson MW, Gomes ALC, Ma Z, Galagan JE, McDonough KA. 2015. Role of intragenic binding of cAMP responsive protein (CRP) in regulation of the succinate dehydrogenase genes Rv0249c-Rv0247c in TB complex mycobacteria. Nucleic acids research 43:5377–93.

21. Morishige Y, Fujimori K, Amano F. 2013. Differential resuscitative effect of pyruvate and its analogues on VBNC (Viable But Non-Culturable) *Salmonella*. Microbes and Environments 28:180–186.

22. Vilhena C, Kaganovitch E, Grünberger A, Motz M, Forné I, Kohlheyer D, Jung K. 2019. Importance of Pyruvate Sensing and Transport for the Resuscitation of Viable but Nonculturable *Escherichia coli* K-12. Journal of bacteriology 201.

23. Yoon JH, Bae YM, Jo S, Moon SK, Oh SW, Lee SY. 2020. Optimization of resuscitation-promoting broths for the revival of *Vibrio parahaemolyticus* from a viable but nonculturable state. Food Science and Biotechnology 30:159.

24. Ortega C, Liao R, Anderson LN, Rustad T, Ollodart AR, Wright AT, Sherman DR, Grundner C. 2014. *Mycobacterium tuberculosis* Ser/Thr Protein Kinase B Mediates an Oxygen-Dependent Replication Switch. PLOS Biology 12:e1001746.

25. Lyon RH, Lichstein HC, Hall WH. 1963. EFFECT OF TWEEN 80 ON THE GROWTH OF TUBERCLE BACILLI IN AERATED CULTURES. Journal of Bacteriology 86:280–284.

26. Huang BX, Kim HY, Dass C. 2004. Probing three-dimensional structure of bovine serum albumin by chemical cross-linking and mass spectrometry. Journal of the American Society for Mass Spectrometry 15:1237–1247.

27. Rombouts I, Lagrain B, Scherf KA, Lambrecht MA, Koehler P, Delcour JA. 2015. Formation and

reshuffling of disulfide bonds in bovine serum albumin demonstrated using tandem mass spectrometry with collision-induced and electron-transfer dissociation. Scientific reports 5:12210.

28. Broersen K, Van Teeffelen AMM, Vries A, Voragen AGJ, Hamer RJ, De Jongh HHJ. 2006. Do sulfhydryl groups affect aggregation and gelation properties of ovalbumin? Journal of agricultural and food chemistry 54:5166–74.

29. Wells AQ. 1937. TUBERCULOSIS IN WILD VOLES. The Lancet 229:1221.

30. Manuse S, Fleurie A, Zucchini L, Lesterlin C, Grangeasse C. 2016. Role of eukaryotic-like serine/threonine kinases in bacterial cell division and morphogenesis. FEMS microbiology reviews 40:41–56.

31. Carette X, Platig J, Young DC, Helmel M, Young AT, Wang Z, Potluri L-P, Moody CS, Zeng J, Prisic S, Paulson JN, Muntel J, Madduri AVR, Velarde J, Mayfield JA, Locher C, Wang T, Quackenbush J, Rhee KY, Moody DB, Steen H, Husson RN. 2018. Multisystem Analysis of *Mycobacterium tuberculosis* Reveals Kinase-Dependent Remodeling of the Pathogen-Environment Interface. mBio 9.

32. Thakur M, Chakraborti PK. 2008. Ability of PknA, a mycobacterial eukaryotic-type serine/threonine kinase, to transphosphorylate MurD, a ligase involved in the process of peptidoglycan biosynthesis. The Biochemical journal 415:27–33.

33. Parikh A, Verma SK, Khan S, Prakash B, Nandicoori VK. 2009. PknB-mediated phosphorylation of a novel substrate, N-acetylglucosamine-1-phosphate uridyltransferase, modulates its acetyltransferase activity. Journal of molecular biology 386:451–64.

34. Jagtap PKA, Soni V, Vithani N, Jhingan GD, Bais VS, Nandicoori VK, Prakash B. 2012. Substrate-bound crystal structures reveal features unique to *Mycobacterium tuberculosis* N-acetyl-glucosamine 1-phosphate uridyltransferase and a catalytic mechanism for acetyl transfer. The Journal of biological chemistry 287:39524–37.

35. Gee CL, Papavinasasundaram KG, Blair SR, Baer CE, Falick AM, King DS, Griffin JE, Venghatakrishnan H, Zukauskas A, Wei J-R, Dhiman RK, Crick DC, Rubin EJ, Sassetti CM, Alber T. 2012. A phosphorylated pseudokinase complex controls cell wall synthesis in mycobacteria. Science signaling 5:ra7.

36. Kang C-M, Nyayapathy S, Lee J-Y, Suh J-W, Husson RN. 2008. Wag31, a homologue of the cell

607 division protein DivIVA, regulates growth, morphology and polar cell wall synthesis in mycobacteria.
608 Microbiology (Reading, England) 154:725–735.
609
610 37. Gupta M, Sajid A, Sharma K, Ghosh S, Arora G, Singh R, Nagaraja V, Tandon V, Singh Y. 2014.
611 HupB, a nucleoid-associated protein of *Mycobacterium tuberculosis*, is modified by serine/threonine
612 protein kinases in vivo. Journal of bacteriology 196:2646–57.
613
614 38. Baronian G, Ginda K, Berry L, Cohen-Gonsaud M, Zakrzewska-Czerwińska J, Jakimowicz D, Molle
615 V. 2015. Phosphorylation of *Mycobacterium tuberculosis* ParB participates in regulating the ParABS
616 chromosome segregation system. PloS one 10:e0119907.
617
618 39. Thakur M, Chakraborti PK. 2006. GTPase activity of mycobacterial FtsZ is impaired due to its
619 transphosphorylation by the eukaryotic-type Ser/Thr kinase, PknA. The Journal of biological
620 chemistry 281:40107–13.
621
622 40. Sureka K, Hossain T, Mukherjee P, Chatterjee P, Datta P, Kundu M, Basu J. 2010. Novel role of
623 phosphorylation-dependent interaction between FtsZ and FipA in mycobacterial cell division. PloS
624 one 5:e8590.
625
626 41. Wright DP, Ulijasz AT. 2014. Regulation of transcription by eukaryotic-like serine-threonine kinases
627 and phosphatases in gram-positive bacterial pathogens. Virulence 5:863–885.
628
629 42. Rock JM, Hopkins FF, Chavez A, Diallo M, Chase MR, Gerrick ER, Pritchard JR, Church GM,
630 Rubin EJ, Sassetti CM, Schnappinger D, Fortune SM. 2017. Programmable transcriptional repression
631 in mycobacteria using an orthogonal CRISPR interference platform. Nature microbiology 2:16274.
632
633 43. Minato Y, Gohl DM, Thiede JM, Chacón JM, Harcombe WR, Maruyama F, Baughn AD. 2019.
634 Genomewide Assessment of *Mycobacterium tuberculosis* Conditionally Essential Metabolic
635 Pathways. mSystems 4.
636
637 44. DeJesus MA, Gerrick ER, Xu W, Park SW, Long JE, Boutte CC, Rubin EJ, Schnappinger D, Ehrt S,
638 Fortune SM, Sassetti CM, Ioerger TR. 2017. Comprehensive Essentiality Analysis of the
639 *Mycobacterium tuberculosis* Genome via Saturating Transposon Mutagenesis. mBio 8.
640
641 45. Sassetti CM, Boyd DH, Rubin EJ. 2003. Genes required for mycobacterial growth defined by high
642 density mutagenesis. Molecular microbiology 48:77–84.
643
644 46. Griffin JE, Gawronski JD, Dejesus MA, Ioerger TR, Akerley BJ, Sassetti CM. 2011. High-resolution

phenotypic profiling defines genes essential for mycobacterial growth and cholesterol catabolism. PLoS pathogens 7:e1002251.

47. Schindelin J, Arganda-Carreras I, Frise E, Kaynig V, Longair M, Pietzsch T, Preibisch S, Rueden C, Saalfeld S, Schmid B, Tinevez J-Y, White DJ, Hartenstein V, Eliceiri K, Tomancak P, Cardona A. 2012. Fiji: an open-source platform for biological-image analysis. Nature Methods 2012 9:7 9:676–682.

48. Garton NJ, Christensen H, Minnikin DE, Adegbola RA, Barer MR. 2002. Intracellular lipophilic inclusions of mycobacteria in vitro and in sputum. Microbiology 148:2951–2958.

49. Weyer K. 1998. Laboratory services in tuberculosis control.Part II. WHO Tech Bull 98:258.

50. Trott O, Olson AJ. 2010. AutoDock Vina: improving the speed and accuracy of docking with a new scoring function, efficient optimization, and multithreading. Journal of computational chemistry 31:455–61.

51. Eberhardt J, Santos-Martins D, Tillack AF, Forli S. 2021. AutoDock Vina 1.2.0: New Docking Methods, Expanded Force Field, and Python Bindings. Journal of chemical information and modeling 61:3891–3898.

52. Berman HM, Westbrook J, Feng Z, Gilliland G, Bhat TN, Weissig H, Shindyalov IN, Bourne PE. 2000. The Protein Data Bank. Nucleic Acids Research 28:235–242.

53. Jumper J, Evans R, Pritzel A, Green T, Figurnov M, Ronneberger O, Tunyasuvunakool K, Bates R, Žídek A, Potapenko A, Bridgland A, Meyer C, Kohl SAA, Ballard AJ, Cowie A, Romera-Paredes B, Nikolov S, Jain R, Adler J, Back T, Petersen S, Reiman D, Clancy E, Zielinski M, Steinegger M, Pacholska M, Berghammer T, Bodenstein S, Silver D, Vinyals O, Senior AW, Kavukcuoglu K, Kohli P, Hassabis D. 2021. Highly accurate protein structure prediction with AlphaFold. Nature 2021 596:7873 596:583–589.

54. Varadi M, Anyango S, Deshpande M, Nair S, Natassia C, Yordanova G, Yuan D, Stroe O, Wood G, Laydon A, Zídek A, Green T, Tunyasuvunakool K, Petersen S, Jumper J, Clancy E, Green R, Vora A, Lutfi M, Figurnov M, Cowie A, Hobbs N, Kohli P, Kleywegt G, Birney E, Hassabis D, Velankar S. 2022. AlphaFold Protein Structure Database: massively expanding the structural coverage of protein-sequence space with high-accuracy models. Nucleic Acids Research 50:D439–D444.

55. Ravala SK, Singh S, Yadav GS, Kumar S, Karthikeyan S, Chakraborti PK. 2015. Evidence that

683 phosphorylation of threonine in the GT motif triggers activation of PknA, a eukaryotic-type
684 serine/threonine kinase from *Mycobacterium tuberculosis*. The FEBS journal 282:1419–31.
685
686 56. Pettersen EF, Goddard TD, Huang CC, Couch GS, Greenblatt DM, Meng EC, Ferrin TE. 2004. UCSF
687 Chimera - A visualization system for exploratory research and analysis. Journal of Computational
688 Chemistry 25:1605–1612.
689
690 57. R Core Team. 2021. R: A Language and Environment for Statistical Computing. 4.1.0. R Foundation
691 for Statistical Computing, Vienna, Austria.
692
693 58. Kanda Y. 2013. Investigation of the freely available easy-to-use software "EZR" for medical statistics.
694 Bone marrow transplantation 48:452–8.
695
696

697 **Figure legends**

698 Figure 1. Viability analyses of DPI-treated Mtb H37Rv

699 (A) Number of culturable cells after DPI treatment. The CFU/mL values were determined
700 by plating the cells onto 7H10 plates in duplicate. Asterisks indicate statistically
701 significant differences (*$p < 0.05$, Welch's *t*-test). Data represent mean ± SD from
702 three independent experiments.
703 (B) Percentage of esterase-active cells after DPI treatment. Approximately 850 cells were
704 counted directly using a 100× objective lens. Data represent mean ± SD from three
705 independent experiments.
706 (C) Fluorescence micrographs of Mtb H37Rv cells stained with carboxyfluorescein
707 diacetate (CFDA) and ethidium bromide (EtBr). Cells stained with CFDA (green)
708 were esterase-positive, and those stained with EtBr (red) were membrane-damaged.
709 Representative images from three individual experiments are shown. Scale bar: 2 μm
710 (D) Percentage of acid-fast-positive cells (open column) or acid-fast-negative but lipid
711 accumulation-positive cells (gray column). Approximately 1,100 cells were counted

712 directly using a 100× objective lens. Data represent mean ± SD from four independent
713 experiments. Asterisks indicate significant differences (***$p < 0.005$, Welch's *t*-test).
714 (E) Merged fluorescence micrographs of Mtb H37Rv cells stained with auramine-O and
715 Nile Red. Cells stained with auramine-O (green) were acid-fast-positive; those stained
716 with Nile Red (red) were acid-fast-negative but lipid accumulation-positive.
717 Representative images from three individual experiments are shown. Scale bar: 2μm
718 (F) Magnified views of Airyscan confocal super-resolution microscopy observations of
719 three different Mtb cells obtained from DPI-treated cultures. Only acid-fast-positive
720 cells (left), both acid-fast-positive and lipid accumulation-positive cells (center,
721 counted as acid-fast-positive), and acid-fast-negative cells with only lipid
722 accumulation-positive cells (right). Dual-positive cells probably represent a transition
723 to a non-culturable state. The indicated foci with arrowheads represent the neutral
724 lipid bodies. Scale bar: 1 μm

725 Figure 2. Reactivation of DPI-treated Mtb H37Rv cells by FBS and OADC supplementation

726 (A) Number of culturable cells on the indicated days of incubation, without
727 supplementation, or supplemented with 2% FBS or 10% OADC in the presence
728 (closed circle) or absence (open circle) of 0.1% BSA. The CFU/mL values were
729 determined by plating the cells onto 7H10 plates in duplicate. Data represent mean ±
730 SD from three independent experiments. U.D. indicates the limit of detection (20
731 CFU/mL).
732 (B) Representative images of regrowth under the indicated conditions were captured at
733 the end of incubation. None, FBS, and OADC represent no supplementation, 2% FBS
734 supplementation, and 10% OADC supplementation, respectively.

735 Figure 3. Effect of human serum albumin, ovalbumin and antioxidants on the reactivation of

736 DPI-treated Mtb.

737 (A) The culturable cells at the end of incubation were supplemented with albumins or
738 antioxidative agents. The CFU/mL values were determined by plating the cells onto
739 7H10 plates in duplicate. Data represent mean ± SD from three independent
740 experiments. Asterisks indicate statistically significant differences between days 0 and
741 20 by Student's *t*-test. (*$p<0.05$)
742 (B) Representative images of regrowth captured at the end of incubation.

743 Abbreviations:
744 BSA, bovine serum albumin; HSA, human serum albumin; OVA, ovalbumin; NAC, N-
745 acetyl-L-cysteine; MAN, D-mannitol.
746 The final concentrations of each reagent were as follows:
747 BSA, HSA, and OVA, 0.1% (w/v); NAC, 500 μM; and MAN, 50 mM.

748 Figure 4. The effect of SQ22536 or H89 or staurosporine on the reactivation of DPI-treated
749 Mtb

750 (A) Number of culturable cells at the end of incubation, supplemented with 0.1% BSA,
751 SQ22536, H89, or staurosporine. Inhibitors were added at the indicated
752 concentrations.
753 (B) Representative images of regrowth captured at the end of incubation.

754 The CFU/mL values were determined by plating the cells onto 7H10 plates in duplicate. Data
755 represent mean ± SD from three independent experiments.

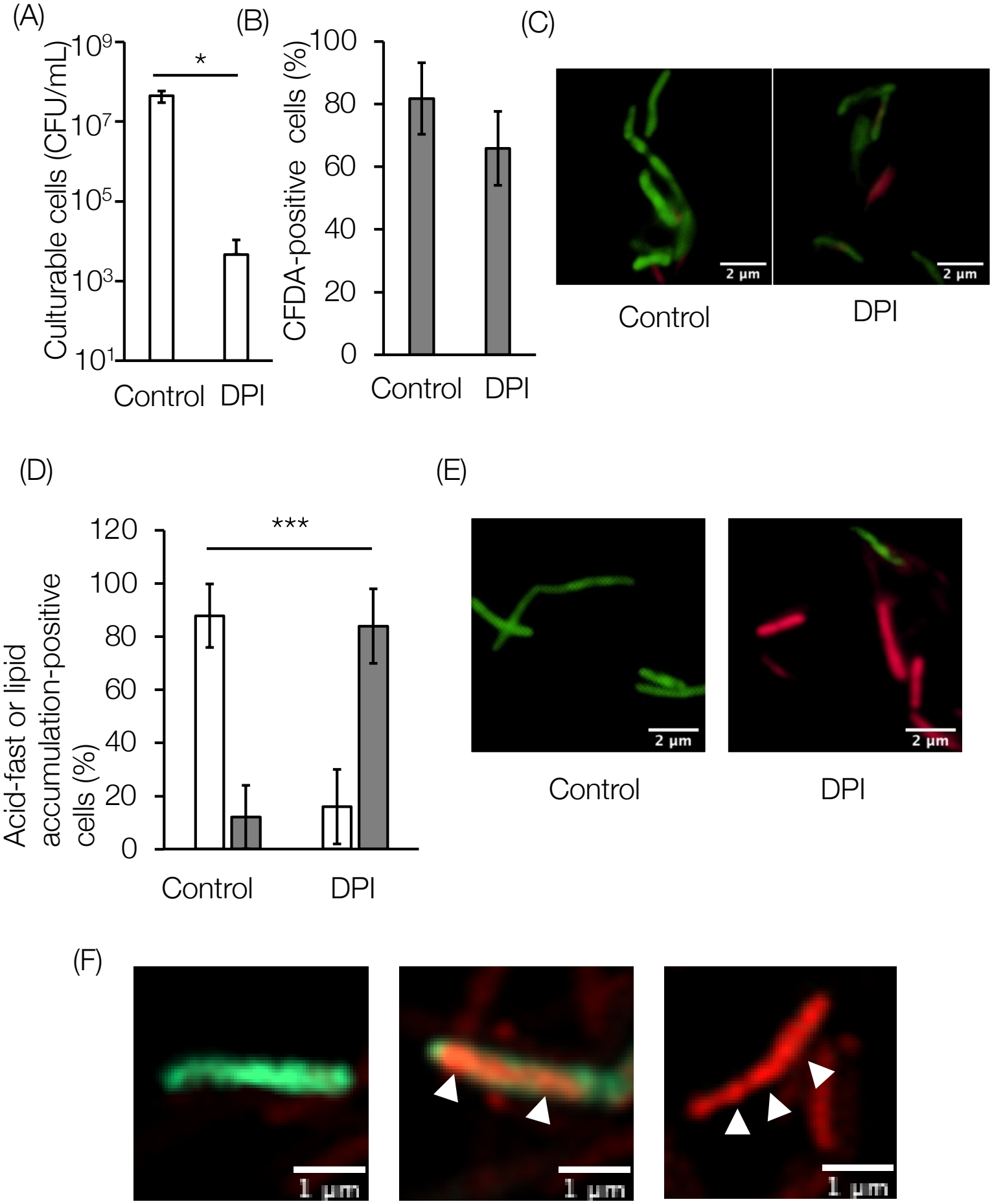
(A)
Culturable cells (CFU/mL)
10^9
10^7
10^5
10^3
10^1
*
Control
DPI
(B)
CFDA-positive cells (%)
100
80
60
40
20
0
Control
DPI
(C)
2 μm
2 μm
Control
DPI
(D)
Acid-fast or lipid accumulation-positive cells (%)
120
100
80
60
40
20
0
***
Control
DPI
(E)
2 μm
2 μm
Control
DPI
(F)
1 μm
1 μm
1 μm

Fig 1.

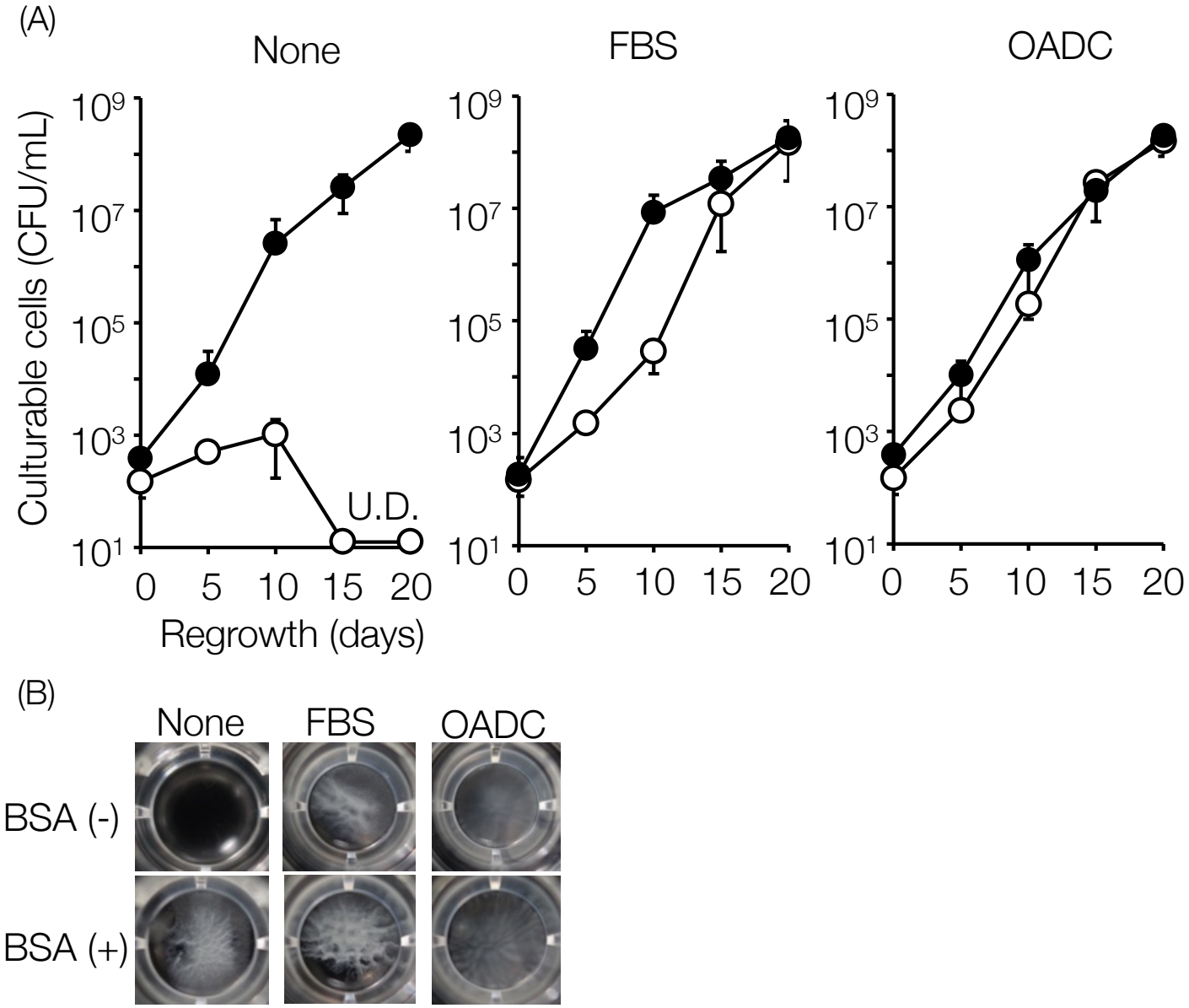
(A)
None
FBS
OADC
Culturable cells (CFU/mL)
10^9
10^7
10^5
10^3
10^1
U.D.
0 5 10 15 20
Regrowth (days)
(B)
None
FBS
OADC
BSA (-)
BSA (+)

Fig 2.

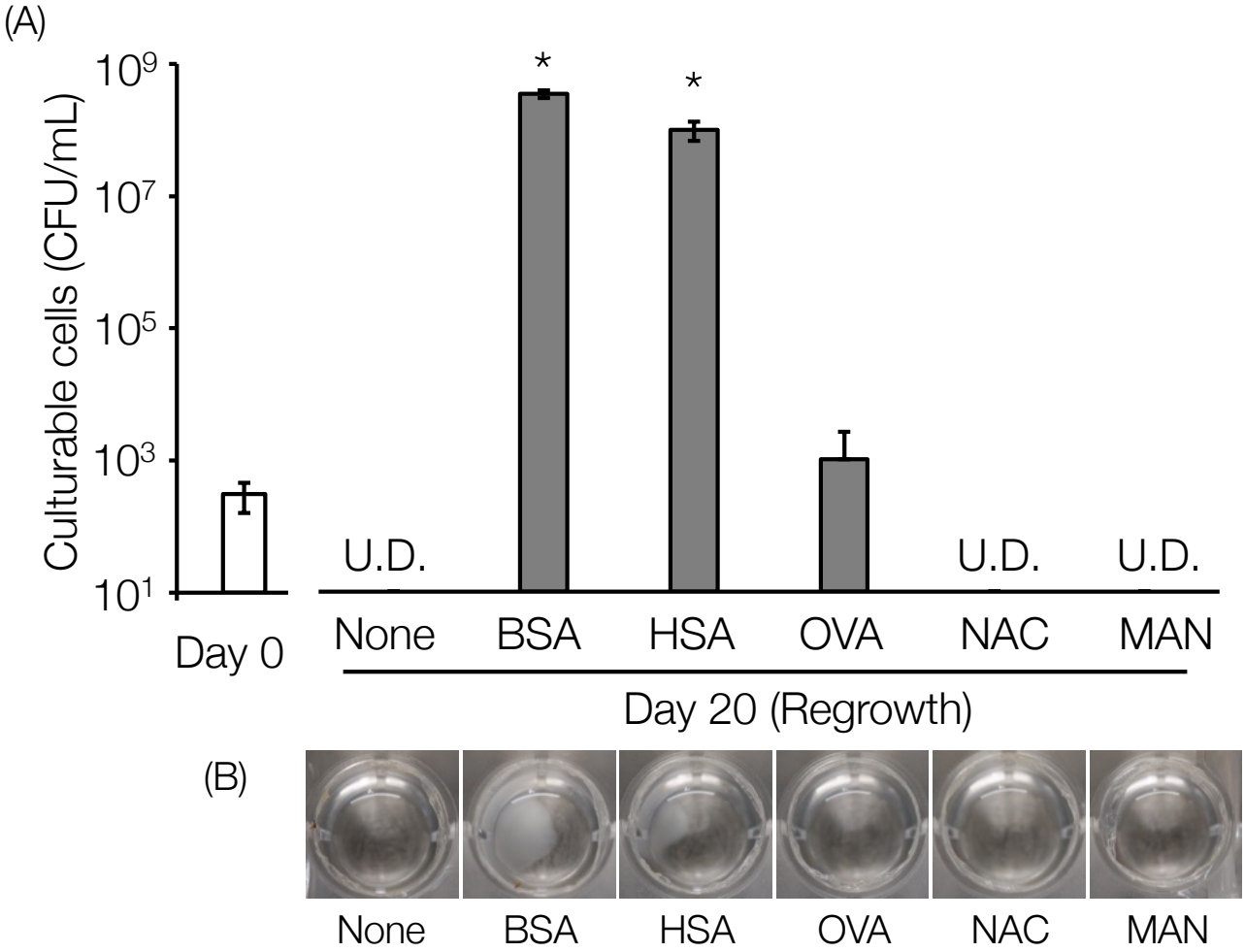
(A)
Culturable cells (CFU/mL)
10^9
10^7
10^5
10^3
10^1
*
*
U.D.
U.D.
U.D.
Day 0
None
BSA
HSA
OVA
NAC
MAN
Day 20 (Regrowth)
(B)
None
BSA
HSA
OVA
NAC
MAN

Fig 3.

(A)

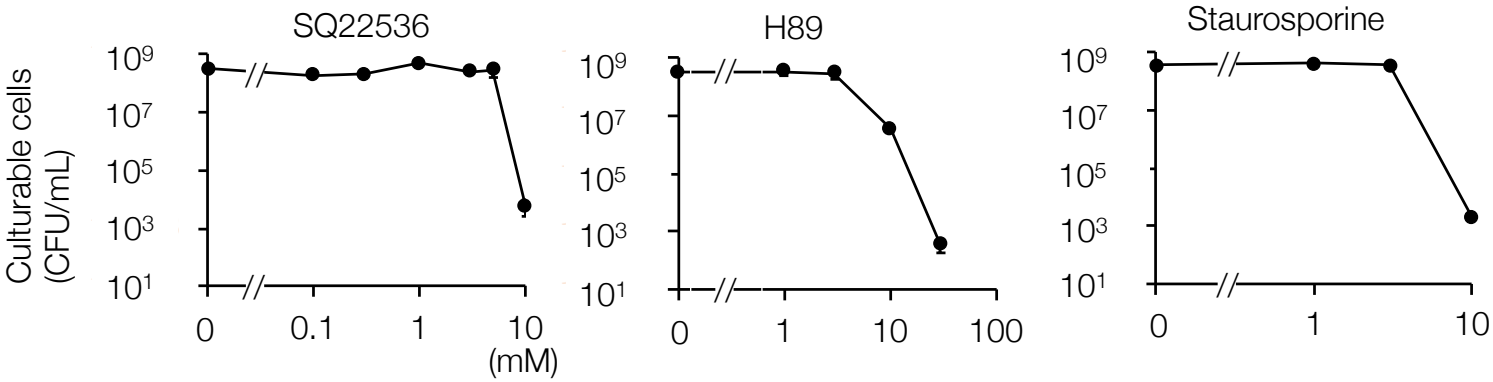
SQ22536
H89
Staurosporine
Culturable cells
(CFU/mL)
10^9
10^7
10^5
10^3
10^1
0
0.1
1
10
100
(mM)

(B)

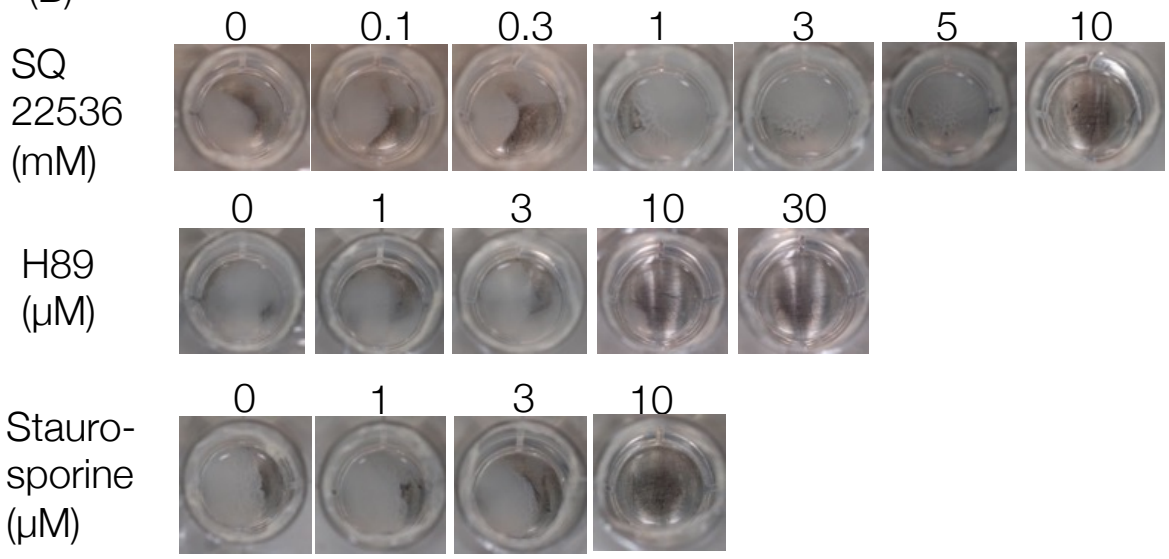
SQ
22536
(mM)
0
0.1
0.3
1
3
5
10
H89
(μM)
0
1
3
10
30
Stauro-
sporine
(μM)
0
1
3
10

Fig 4.